

Polymer Chemistry

Accepted Manuscript



This is an *Accepted Manuscript*, which has been through the Royal Society of Chemistry peer review process and has been accepted for publication.

Accepted Manuscripts are published online shortly after acceptance, before technical editing, formatting and proof reading. Using this free service, authors can make their results available to the community, in citable form, before we publish the edited article. We will replace this *Accepted Manuscript* with the edited and formatted *Advance Article* as soon as it is available.

You can find more information about *Accepted Manuscripts* in the [Information for Authors](#).

Please note that technical editing may introduce minor changes to the text and/or graphics, which may alter content. The journal's standard [Terms & Conditions](#) and the [Ethical guidelines](#) still apply. In no event shall the Royal Society of Chemistry be held responsible for any errors or omissions in this *Accepted Manuscript* or any consequences arising from the use of any information it contains.

ARTICLE

Tuning of HOMO energy levels and open circuit voltages in solar cells based on statistical copolymers prepared by ADMET polymerization†

Cite this: DOI: 10.1039/x0xx00000x

Received 00th January 2012,
Accepted 00th January 2012

DOI: 10.1039/x0xx00000x

www.rsc.org/polymers

Bryan D. Paulsen,^a Joshua C. Speros,^b Megan S. Claflin,^c Marc A. Hillmyer*^b and C. Daniel Frisbie*^a

A series of donor-acceptor statistical copolymers based on a 2,7-divinyl-9,9'-di-*n*-hexylfluorene (FV) donor and 4,7-bis(4-hexadecyl-5-propenyl-2-thienyl)-2,1,3-benzothiadiazole (TBTV) acceptor were prepared to investigate the relationship between copolymer donor-acceptor ratio and organic solar cell (OSC) performance. Homopolymers of the donor and acceptor moieties were prepared by acyclic diene metathesis (ADMET) methods. Five copolymers with systematically varied donor-acceptor ratios spanning the entire composition range were also prepared. All homopolymers and copolymers were characterized using size exclusion chromatography, nuclear magnetic resonance spectroscopy, ultraviolet-visible spectroscopy, and electrochemical cyclic voltammetry. Additionally, each polymer was incorporated into thin film field effect transistor and photovoltaic devices to investigate optoelectronic properties. The highest occupied molecular orbital (HOMO) level was found to be tunable over a 600 meV range through systematic variation of the copolymer donor-acceptor ratio. This same tunability manifested in solar cell open circuit voltage (V_{oc}), which also varied over a 600 mV range. Short circuit current density (J_{sc}) correlated well with field effect hole mobility. This series exemplifies the relationship between copolymer composition, HOMO energy level, and V_{oc} , and demonstrates that peak solar cell performance can be achieved at non-stoichiometric donor-acceptor compositions.

Introduction

As research in polymer-fullerene bulk heterojunction (BHJ) organic solar cells (OSCs) approaches the end of a second decade,¹ interest remains high due to its promising potential as a large scale, low cost source of renewable energy.² The development of donor-acceptor (D-A) conjugated copolymers has led to a rapid improvement in OSC performance with both single and tandem junction power conversion efficiencies (PCE) hovering around 10%.³⁻⁶ To achieve such performance, tunability of the D-A copolymer properties has become a necessity. Specifically, precise control over the copolymer frontier molecular orbital energy levels has been key to obtaining the narrow optical band gaps (E_g^{opt}) and deep highest occupied molecular orbital (HOMO) levels required for the realization of high photovoltaic performance.^{7,8}

Traditionally, energy level tuning in the donor polymer has been accomplished by combining various donor and acceptor moieties in the backbone and further modifying the side chain

functionalization of these subunits.^{7,8} In nearly all cases, alternating D-A copolymers with stoichiometric amounts of the donor and acceptor have been studied. However, some OSC studies have focused on statistical copolymers to introduce side chain variation⁹ and to produce non-stoichiometric D-A copolymers,¹⁰⁻¹³ terpolymers,¹⁴⁻¹⁶ and beyond.¹⁷ The limited attention given statistical copolymerization is in part due to the added synthetic complexity required. Employing traditional polymerization routes (e.g., Stille and Suzuki couplings) requires three monomers¹⁰⁻¹³ or the preparation of hetero-difunctional monomers.^{14,15} A powerful alternative to the generation of statistical copolymers is acyclic diene metathesis (ADMET) polymerization. ADMET polymerization combines olefinic functionalities and has been used to control copolymer composition by variation of the monomer feed ratio.^{18,19} Using this method, statistical copolymerization throughout the range of possible D-A copolymer composition has established the broad tunability of E_g^{opt} and molecular orbital energy levels.¹⁹

The recognized relationship between HOMO level depth and solar cell open circuit voltage (V_{oc}) suggests that statistical D-A copolymerization should allow direct synthetic control over solar cell V_{oc} . However, studies of D-A copolymers covering the entire composition window have yet to be extended to OSCs.

Here we investigate the OSC performance of a series of statistical D-A copolymers spanning the entire composition window. An idealized polymer for photovoltaic applications should have an E_g^{opt} of 1.3–1.8 eV and a HOMO level of -5.4 – -5.8 eV.²⁰ Thus, a donor that contributes to a deep HOMO and an acceptor that allows for a narrow band gap are desired. Fluorene (FV) and dithiophene benzothiadiazole (TBTv) derived diolefinic monomers were selected as the donor and acceptor, respectively, for the ADMET synthesis. In this work, molar mass and D-A composition in the product polymers were determined by size-exclusion chromatography (SEC) and nuclear magnetic resonance (NMR), respectively. Copolymer energy level positions were investigated with cyclic voltammetry (CV) and ultraviolet–visible (UV–vis) spectroscopy allowing the construction of a D-A copolymer composition dependent energy level diagram. Hole mobility was investigated in field effect transistors (FETs). BHJ OSCs were prepared to evaluate photovoltaic parameters and establish the utility of controlling D-A copolymer composition to tune solar cell V_{oc} .

Materials and methods

2,7-Divinyl-9,9'-di-n-hexylfluorene (FV)^{18,21} and 4,7-bis(4-hexadecyl-5-propenyl-2-thienyl)-2,1,3-benzothiadiazole (TBTv)¹⁹ were prepared according to previous work. The commercially available solvents and reagents for these syntheses were used as received from Sigma Aldrich and Acros Organics. Degassed tetrahydrofuran (THF) was purified by passage through an activated alumina column and collected in flame-dried, air-free flasks. 1,2,4-trichlorobenzene (TCB) was degassed with argon and distilled under vacuum. All reactions were performed under argon or vacuum using standard Schlenk techniques.

Poly(3,4-ethylenedioxythiophene):poly(styrenesulfonate) (PEDOT:PSS, Clevios P VP Al 4083, aqueous dispersion) and [6,6]-phenyl C₇₁ butyric acid methyl ester (PC₇₀BM) were purchased from Heraeus Materials Technology (West Conshohocken, PA) and American Dye Source (Baie-d'Urfé, Quebec), respectively.

UV–vis absorption spectra for polymer solutions and thin films were acquired on a Spectronic Genesys 5 spectrometer over a wavelength range of 300–1000 nm. The solution spectra were obtained in a 1 cm quartz cuvette, and the film spectra were obtained by spin casting a 1,2-dichlorobenzene solution (10 mg mL⁻¹, 2000 rpm, 60 s) on a glass substrate. CV was run using a Pine Instruments bipotentiostat with a Pt wire mesh counter electrode, an Ag wire pseudo-reference electrode, and Au-coated glass working electrode. Polymers were spin-coated onto the working electrode from a 1,2-dichlorobenzene solution, and voltammograms were recorded in the ionic liquid 1-butyl-1-methylpyrrolidinium

bis(trifluoromethylsulfonyl)amide, [P14][TFSA], at a scan rate of 50 mV sec⁻¹. HOMO levels were estimated from the oxidation onset relative to cobaltocene using the equation: $E_{HOMO} = -q(E_{ox, onset vs. Cc o/+} + 3.75)$.

OSC fabrication began with patterned ITO substrates (Delta Technologies (Stillwater, MN), sheet resistance 8–12 ohms sq⁻¹), which were successively sonicated for 10 min each in acetone, methanol (MeOH), and isopropyl alcohol (IPA). The substrates were blown dry with N₂ between each sonication. This was followed by a 10 min UV/O₃ exposure, directly followed by PEDOT:PSS spin-coating at 2000 revolutions min⁻¹ (rpm) from an aqueous suspension diluted 1:1 (v/v) with MeOH. PEDOT:PSS coated substrates were then transferred to a glove box and dried on a hot plate at 130 °C for 20–30 minutes. All remaining fabrication steps were carried out in a N₂ glove box. Active layers were deposited by spin-coating a 1:4 polymer:fullerene solution with a total concentration of 40 mg mL⁻¹ in dichlorobenzene. Spin-coating was carried out in a glove box at 1000 rpm for 60 seconds. Active layer films were dried slowly in covered petri dishes at ambient temperature. An additional hole-blocking layer was formed by spin-coating a 5 mg mL⁻¹ (EtOH) TiO₂ nanoparticle suspension at 4000 rpm for 60 seconds. Devices were capped with aluminum cathodes, ca. 100 nm as measured by quartz crystal microbalance, via thermal evaporation at a rate of 2–3 Å min⁻¹. Silver paste was applied to the anode and cathode contact pads facilitating ohmic contact with the testing apparatus. PV current-voltage characteristics were collected using an Agilent 4155C semiconductor parameter analyzer, under dark conditions and simulated solar illumination using a 150 W Xe-arc lamp (Oriol) with an AM 1.5 G filter, attenuated to 100 mW cm⁻². Solar cell measurements were made on at least one batch of 6 devices and in some cases two batches for a total of 12 devices.

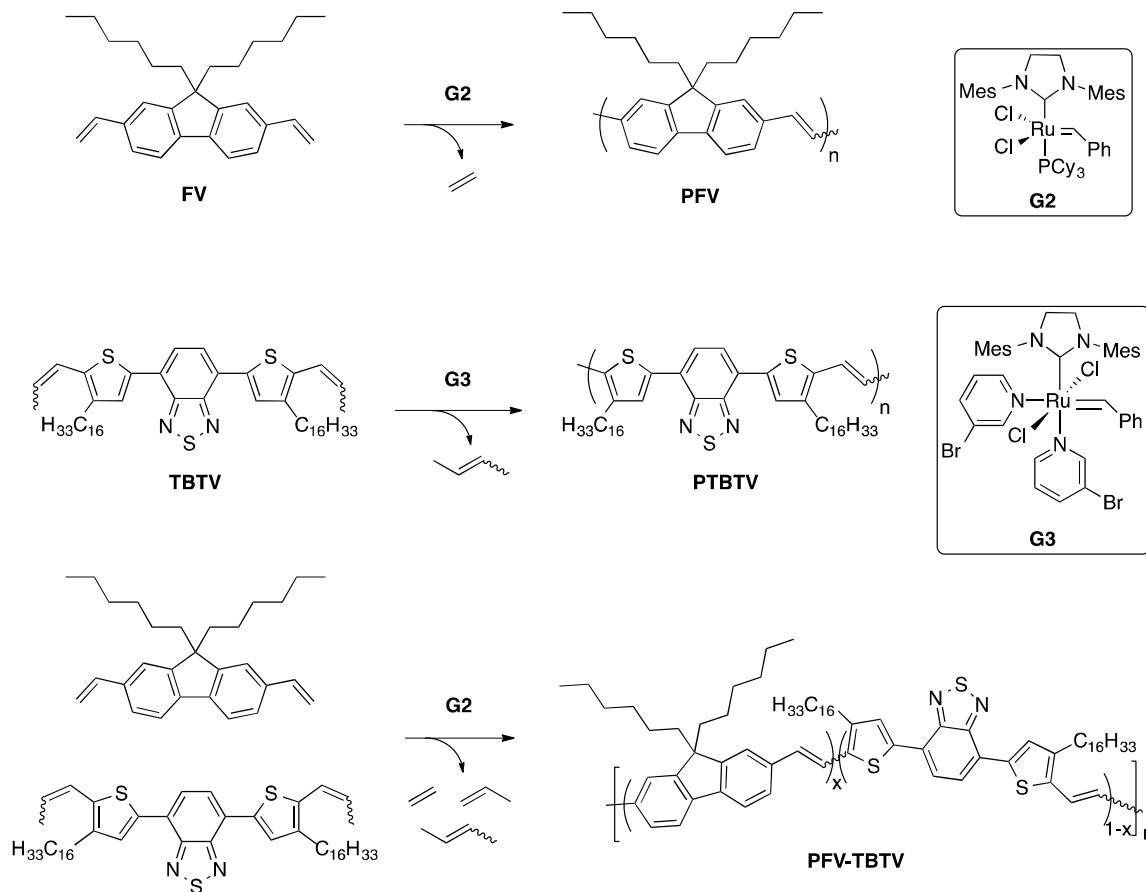
Bottom gate bottom contact geometry FETs were fabricated on doped Si wafers with 3000 Å of thermally grown oxide. Gold source-drain contacts, ca. 250 Å as measured by quartz crystal microbalance, were deposited via electron beam evaporation (Temescal) of a 25 Å chromium adhesion layer and 225 Å of gold, and patterned via the lift-off technique. Substrates were cleaned with successive acetone, MeOH, and IPA sonications followed by a UV/O₃ exposure. In a N₂ glove box, substrates were treated with n-octadecyltrichlorosilane (OTS) to improve polymer film formation. Polymer active layers were spin-coated from 10 mg mL⁻¹ 1,2-dichlorobenzene solutions at 2000 rpm, and baked on a hot plate at 105 °C for 10 min to drive off residual solvent. Transistors were tested in a Desert Cryogenics vacuum probe station at room temperature housed within a N₂ glove box. Output and transfer curves were collected with Keithley 236, 237, and 6517A source meters controlled by a computer using customized LabView code.

Results and discussion

Polymer synthesis

Both homopolymers and copolymers (Scheme 1) were prepared by ADMET polymerization using N-heterocyclic carbene functionalized ruthenium metathesis catalysts (G2^{22,23} and G3²⁴). In our previous study we utilized dipropenyl monomers as they were less susceptible to decomposition and side reactions due to the ethylidene-ruthenium intermediates.^{19,25–27}

However, prior literature demonstrated the successful ADMET polymerization of FV (divinyl) using G2 to give high molecular weight species without deleterious side reactions.^{28,29} Given this information we utilized FV and emphasized use of the more robust G2 for this study.



Scheme 1 Homopolymer (PFV, PTBTv) and copolymer (PFV-TBTv) synthesis.

All polymerizations were conducted under reduced pressure (20–50 mTorr) in anhydrous 1,2,4-trichlorobenzene with G2/G3 (1–2 mol%). After polymerization for 15–48 h reactions were quenched by the addition of ethyl vinyl ether and precipitated into a non-solvent (MeOH or acetone). Polymers were purified by Soxhlet extraction with the same non-solvent used for precipitation (see ESI†).

Polymer characterization

Relative polymer molar masses were determined by SEC in chloroform versus polystyrene standards. PFV and PTBTv homopolymers reached number average molecular weights (M_n) of 6.0 and 6.9 kg mol⁻¹, respectively (Table 1). Interestingly, the M_n values of all PFV-TBTv copolymers exceeded those of the homopolymers. The FV:TBTV ratios in isolated copolymers (a–e) were quantified using ¹H NMR

spectroscopy (see ESI Fig. S4†) and were near the feed ratios in all cases (Table 1). Although the *cis/trans* ratio was not determined, all backbone olefins were assumed to be *trans* based on spectroscopic analysis for related polymers reported in a previous publication.³⁰ Copolymer molar mass was observed to increase with increasing FV content. This was expected as the less sterically hindered divinyl monomer FV will polymerize more readily than the dipropenyl TBTV. This may also be due to the enhanced solubility of the resultant copolymers with higher FV fractions. Although it could not be confirmed spectroscopically, it is reasonable to assume that because of this inherent difference in polymerizability the copolymer sequence distribution could be gradient-like initially. However, the long polymerization times employed likely allow ample time for cross metathesis and sequence randomization.

ARTICLE

Table 1 NMR, SEC, UV-vis, and CV data for homo- and copolymers

sample ID ^a	observed ratio ^b	M_n (kg/mol) ^c	\bar{D}^c	$\lambda_{\max, \text{film}}^1$ (nm) ^d	$\lambda_{\max, \text{film}}^2$ (nm)	E_g^{opt} (eV) ^e	HOMO (eV) ^f
PFV	–	6.0	2.8	427(456)	–	2.59	-5.85
PTBTv	–	6.9	1.9	430	682	1.49	-5.28
PFV-TBTv	FV:TBTv						
a (80:20)	77:23	38.8	2.5	429(454)	574	1.77	-5.81
b (60:40)	61:39	31.2	2.3	430(453)	591	1.65	-5.62
c (50:50)	52:48	21.9	2.3	430	610	1.58	-5.60
d (40:60)	42:58	13.0	1.8	430	607	1.57	-5.51
e (20:80)	23:77	8.4	1.7	430	640	1.51	-5.42

^aValues in parentheses are monomer feed ratios. ^bDetermined by integration of appropriate resonances in ¹H NMR spectra. ^cDetermined by SEC in CHCl₃ versus polystyrene standards. ^dPolymer film spin-coated from CHCl₃ onto glass substrates; values in parentheses are secondary peaks/shoulders. ^eDetermined from onset absorption of thin film ($E_g^{\text{opt}} = 1240 \text{ (nm eV)}/\lambda_{\text{onset}} \text{ (nm)}$). ^fDetermined from onset electrochemical oxidation of thin film ($E_{\text{HOMO}} = (E_{\text{onset,ox vs Cc+/o}} + 3.75) \text{ eV}$).

Optical and electrochemical behavior

Optical behavior was studied in dilute chloroform solutions (see ESI Fig. S5[†]) and in spin-coated thin films by UV-vis spectroscopy (Figure 1). PFV homopolymer films displayed absorption maxima (λ_{\max}) at 427 nm, and an absorption shoulder at 457 nm due to order induced vibronic coupling. PTBTv displayed two distinct absorption maxima centered at 430 and 682 nm. The first and smaller λ_{\max} at 430 nm was attributed to the π - π^* transition, while the principal absorption was possibly a result of intramolecular charge transfer.³¹ Optical band gap (E_g^{opt}) values were determined from the onset of absorption (λ_{onset}) in the polymer thin film ($E_g^{\text{opt}} = 1240/\lambda_{\text{onset}}$). The λ_{onset} of electron-rich PFV homopolymer at 479 nm corresponded to an E_g^{opt} of 2.59 eV, while the electron deficient PTBTv homopolymer λ_{onset} of 832 nm yielded an E_g^{opt} of 1.49 eV. The large difference in homopolymer E_g^{opt} potentially provides an 1100 meV range over which the E_g^{opt} can be tuned through composition control of the PFV-TBTv statistical copolymer.

In the PFV-TBTv copolymers, λ_{\max}^1 (FV absorption) appeared pinned around 430 nm, independent of copolymer composition, with the relative FV absorption being suppressed with increasing TBTv concentration. Conversely, the position of λ_{\max}^2 (TBTv absorption) scaled with TBTv concentration, varying from 682 nm in the homopolymer to 574 nm in the 77:23 FV:TBTv copolymer (**a**). As with the homopolymers, copolymer E_g^{opt} was determined from the onset of optical absorption. Initial incorporation of TBTv (~20% TBTv monomer) led to a precipitous decrease in E_g^{opt} (820 meV) relative to the PFV homopolymer, and further decreased with increasing TBTv concentration. This is analogous to previous results with thienylene vinylene-TBTv copolymers.¹⁹ Such non-linear E_g^{opt} dependence on TBTv ratio is advantageous as all the copolymers in this series yielded low band gaps ($E_g^{\text{opt}} <$

1.8 eV) desirable for photovoltaic applications. Thus, E_g^{opt} was found to be synthetically tunable through statistical copolymerization, especially over the range of band gaps of interest in photovoltaic cells. All polymers were of high enough molar mass that conjugation length and E_g^{opt} were assumed saturated.³²

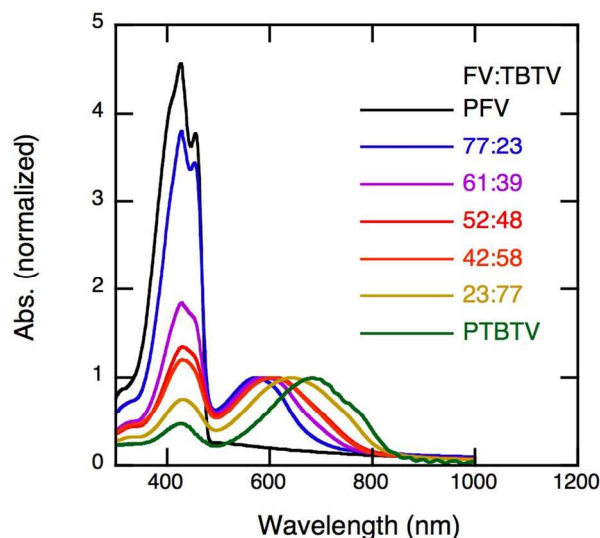


Figure 1 UV-vis film spectra of the PFV-TBTv series and corresponding homopolymers. All spectra, except PFV, normalized to the second (TBTv) absorption peak.

To establish the absolute energy level positions of the frontier molecular orbitals, which give rise to the tunable E_g^{opt} of this copolymer system, the HOMO levels were determined by measuring the onset of electrochemical oxidation. The oxidation onset was determined by CV carried out in a room temperature ionic liquid electrolyte known for a broad voltage window of electrochemical stability and high sweep-to-sweep reproducibility.³³ Homo- and copolymers were spin-coated on

gold working electrodes and displayed clear and reproducible electrochemical oxidation (see ESI Fig. S6†). Of the series investigated, the PTBTV homopolymer exhibited the earliest onset of electrochemical oxidation at 1.48 V vs $Cc^{+/0}$. Copolymer oxidation onsets steadily moved further positive with decreasing TBTV composition, with the neat PFV displaying the furthest positive onset of oxidation at 2.10 V vs $Cc^{+/0}$. The measured reference potentials for each sample were internally calibrated using the standard redox couple cobaltocenium hexafluorophosphate ($CcPF_6$) known to undergo a reversible reduction at -1350 mV vs the ferrocene redox couple in ionic liquids.^{34,35} Based on the most commonly accepted ferrocene oxidation potential of 5.1 eV below vacuum level,³⁶ the HOMO level depths were determined by $E_{HOMO} = -(E_{(onset,ox\ vs\ Cc^{+/0})} + 3.75)$ eV. Consequently, the calculated HOMO levels for the series steadily varied from -5.28 to -5.85 eV (Table 1), demonstrating a window of nearly 600 meV through which the HOMO levels were synthetically tunable by varying the copolymer D-A composition.

Copolymer composition dependent energy level diagram

Using the E_g^{opt} and HOMO level depths, an energy level diagram for the series was constructed (Figure 2a). Lowest occupied molecular orbital (LUMO) level positions were estimated by adding the E_g^{opt} to the HOMO level position. The energy level diagram shows clearly the direct tunability of the HOMO level through control of D-A composition. The LUMO of the copolymers varies by only ~130 meV, and in a less systematic manner. Again, the presence of TBTV in the copolymers leads to uniformly narrow E_g^{opt} and likely contributes to the relative immobility of the LUMO. The chemically modified fullerenes [6,6]-phenyl C_{61} butyric acid methyl ester ($PC_{60}BM$) and [6,6]-phenyl C_{71} butyric acid methyl ester ($PC_{70}BM$) are known to share identical onsets of electrochemical reduction,³⁷ and thus identical LUMO level positions of 4.3 eV.²⁰

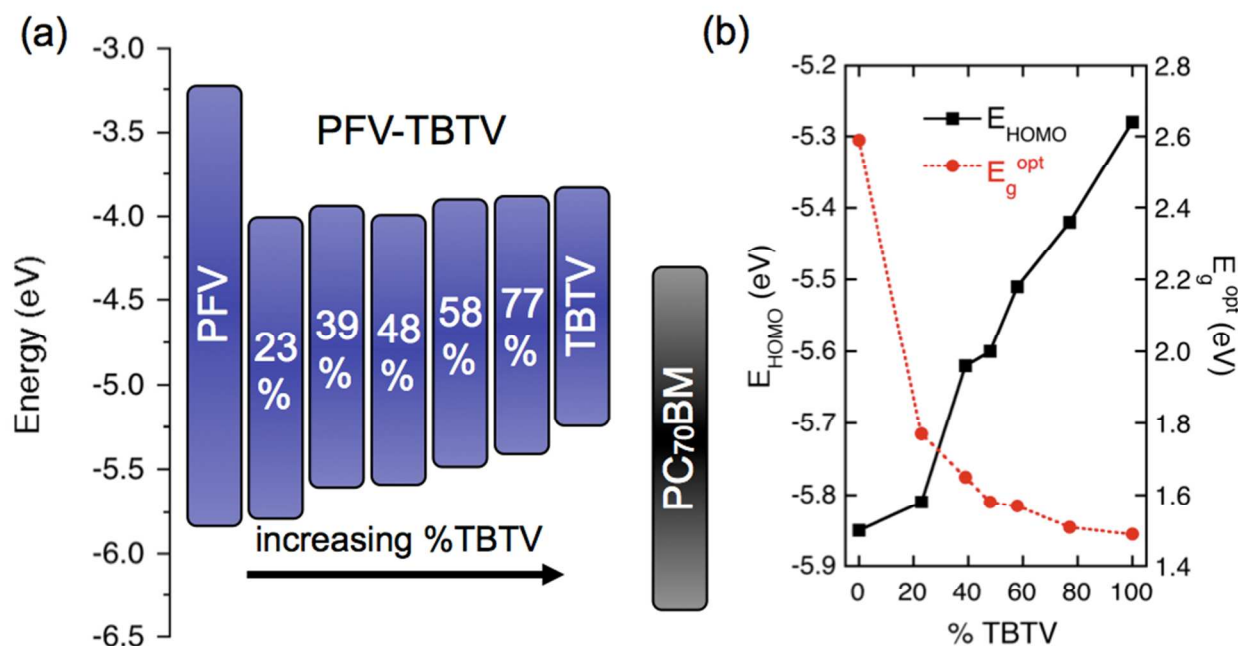


Figure 2 (a) Energy level diagram of PFV, PFV-TBTV copolymers (showing mol% incorporated TBTV monomer), PTBTV, and $PC_{70}BM$ for reference. (b) E_{HOMO} and E_g^{opt} versus polymer composition.

BHJ solar cell and FET performance

To evaluate the effect of synthetically tuned HOMO level on photovoltaic behavior, homo- and copolymers were blended with chemically modified fullerene, $PC_{70}BM$, in a 1:4 polymer:fullerene ratio to form the active layer in BHJ solar cell devices (Figure 3a), with the device performance parameters summarized in Table 2. The most apparent trend was the progression of V_{oc} to higher potential with increasing FV content, ranging from ~0.3 to ~0.9 V. Plotting V_{oc} versus the electrochemically determined HOMO level (Figure 3b)

further illustrates the important role of the HOMO level in determining V_{oc} . In fact, the ~600 meV range of tuned HOMO levels is matched by the ~600 mV range in measured V_{oc} , confirming the direct tunability of V_{oc} through statistical copolymer composition. This result is intuitive, as the V_{oc} should depend on the difference between the polymer HOMO and the fullerene LUMO. Brabec *et al.* originally fit this relationship as $V_{oc} = 1/e(|E_{HOMO}^{Poly}| - |E_{LUMO}^{Full}|) - E_{loss}$, where E_{loss} represents voltage losses in the diode.²⁰ In our case the systematic E_{loss} was found to be ~600 mV, which is consistent with contemporary values of ~550 mV.^{38–40}

ARTICLE

Table 2. Photovoltaic performance data for homo- and copolymers

sample ID ^a	observed ratio ^b	J_{sc} (mA cm ⁻²) ^c	V_{oc} (V) ^c	FF ^c	PCE (%) ^c
PFV	–	5.75 ± 0.07	0.915 ± 0.006	0.330 ± 0.005	1.74 ± 0.02
PTBTV	–	1.42 ± 0.18	0.303 ± 0.023	0.315 ± 0.015	0.14 ± 0.05
PFV-TBTV	F:TBT				
a (80:20)	77:23	4.91 ± 0.05	0.920 ± 0.005	0.370 ± 0.004	1.67 ± 0.03
b (60:40)	61:39	7.42 ± 0.14	0.852 ± 0.004	0.416 ± 0.002	2.63 ± 0.05
c (50:50)	52:48	7.01 ± 0.11	0.780 ± 0.005	0.377 ± 0.004	2.06 ± 0.05
d (40:60)	42:58	4.90 ± 0.18	0.682 ± 0.004	0.323 ± 0.007	1.08 ± 0.05
e (20:80)	23:77	6.46 ± 0.04	0.530 ± 0.005	0.499 ± 0.006	1.71 ± 0.02

^aValues in parentheses are monomer feed ratios. ^bDetermined by integration of appropriate resonances in ¹H NMR spectra. ^cAll values averaged from multiple devices with error ranges reflecting one standard deviation.

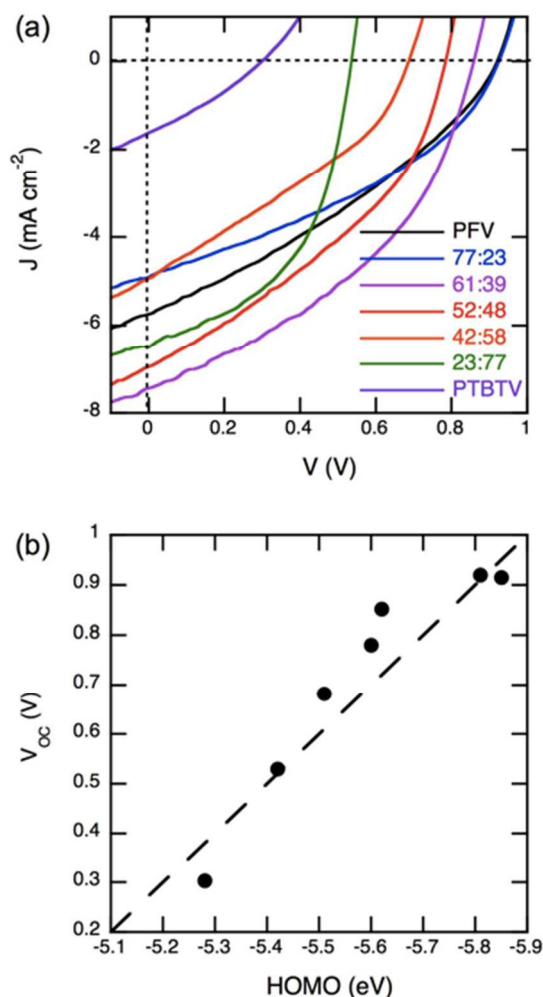


Figure 3 (a) Representative J - V characteristics of PFV, PFV-TBTV copolymers, and PTBTV solar cells with a 1:4 copolymer:PC₇₀BM active layer, under simulated AM 1.5 spectrum and (b) measured V_{oc} (solid circles) versus HOMO level depth. Dotted dotted line represents an approximately linear variation of V_{oc} with HOMO level depth.

Unlike V_{oc} , J_{sc} showed no direct relationship with copolymer composition. Copolymer **b** (61:39 FV:TBT) devices reached the highest values at 7.42 ± 0.14 mA cm⁻² (Figure 4a). Excluding PTBTV (1.42 ± 0.18 mA cm⁻²), the rest of the series produced J_{sc} values between 4 and 7 mA cm⁻².

In order to elucidate the non-monotonic dependence of J_{sc} on copolymer composition, transistors were made based on the polymers to investigate the effects of tuned energy levels on hole transport. Bottom gate, bottom contact devices were fabricated with an OTS monolayer treated silicon dioxide gate dielectric. Transfer and output curves were collected for each sample, with the hole mobility (μ_h) and threshold voltage (V_t) extracted from the saturation regime of transistor operation. Good field effect behavior was observed, with μ_h varying from $\sim 10^{-4}$ to $\sim 10^{-3}$ cm² V⁻¹ s⁻¹ and closely matching measured D-A composition dependent J_{sc} behavior (Figure 4a). Likewise V_t varied from ~ 50 down to ~ 5 V, roughly matching the E_{HOMO} behavior (see ESI Fig. S7[†]). As with J_{sc} , the extracted μ_h varied non-monotonically with copolymer composition, displaying peaks at 39 and 77% TBTV monomer (copolymers **b** and **e**). To confirm these results, multiple trials of multiple devices were carried out for each copolymer sample, with the statistical precision reflected in the error bars in Figure 4a. The existence of local J_{sc} and μ_h maxima on either side of a 50:50 D-A composition was surprising and it has interesting implications in a field where non-stoichiometric copolymer donor-acceptor compositions are not often studied. Overall, however, the correlation of J_{sc} and μ_h is satisfying as it supports the interpretation that hole transport efficiency is the underlying cause of the dependence of J_{sc} on composition.

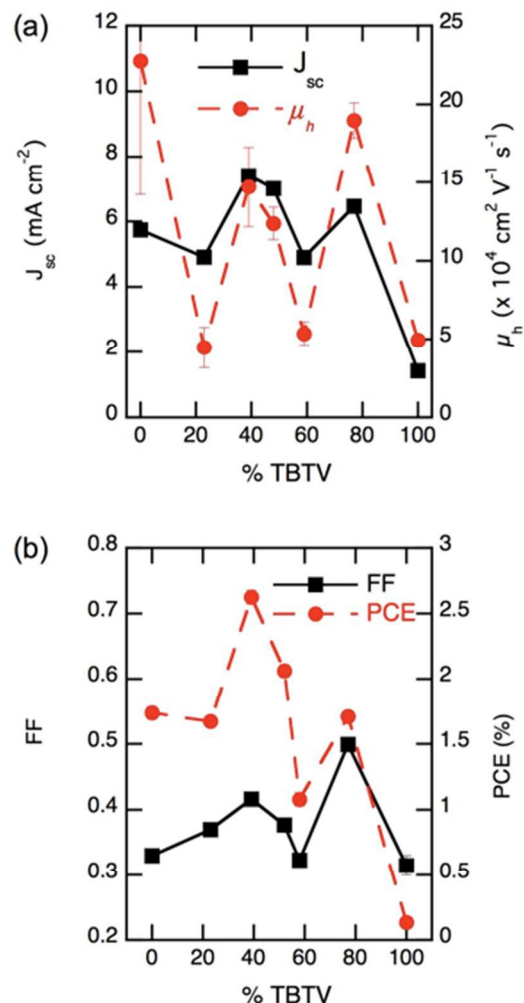


Figure 4 (a) Solar cell J_{sc} and field effect hole mobility, and (b) solar cell FF and PCE as a function of incorporated TBTV (mol%).

Usually carrier mobility and solar cell performance improve with increased molar mass of the donor polymer.^{19,41–49} Here, J_{sc} and μ_h showed no correlation with molecular weight. In fact, the highest molecular weight sample (77:23 FV:TBTV) yielded the lowest μ_h , while the lowest molecular weight yielded sample (PFV) the highest μ_h . Clearly in this case structural and energetic factors trumped the effect of polymer chain length. Despite the low molar mass of neat PFV, the thin film UV–vis spectra displayed very strong vibronic structure common in highly ordered high mobility polymers.¹⁹ Thus, relatively high μ_h was not unanticipated.

The copolymer composition dependent fill factor (FF) ranged between 0.3 and 0.5, also peaking at compositions that displayed μ_h maxima. This is reasonable as μ_h is one of the many factors that influence FF,⁵⁰ and a previous study of fluorene and benzothiadiazole based copolymers has shown that FF is especially sensitive to μ_h .⁵¹

Overall photovoltaic device power conversion efficiency (PCE) did not show a direct correlation with D-A composition (Figure 4b), but instead must be understood in terms of the contributing factors. The 52:48 FV:TBTV (c) based devices produced a PCE of $2.06 \pm 0.05\%$. This performance was in line with other fluorene and benzothiadiazole incorporating perfectly alternating (i.e. 50:50) D-A copolymers, with non-vinyl analogues consistently reporting $\sim 2.5\%$ efficiency,^{46,52,53} and vinyl analogues reporting 1.5% efficiency.⁵⁴ This is especially encouraging, as previous vinyl analogues often underperformed by a factor of four compared to their non-vinyl equivalents.^{19,55–57} Photovoltaic devices incorporating the slightly donor rich copolymer **b** (61:39 FV:TBTV) improved PCE, delivering $2.63 \pm 0.05\%$ efficiency due to increased μ_h (higher J_{sc}) and a deeper HOMO level (higher V_{oc}). This was the best photovoltaic performance of the series, and occurred at a D-A copolymer composition other than the commonly studied 50:50.

The acceptor rich 23:77 FV:TBTV copolymer (e) displayed a very narrow E_g^{opt} (1.51 eV) and a high μ_h ($1.9 \pm 0.1 \times 10^{-3} \text{ cm}^2 \text{ V}^{-1} \text{ s}^{-1}$), which gave rise to a high J_{sc} ($6.46 \pm 0.04 \text{ mA cm}^{-2}$). In turn, the high μ_h and J_{sc} values gave rise to a strong FF (0.50 ± 0.02). However, the large acceptor concentration yielded a relatively shallow HOMO level (-5.42 eV), which limited V_{oc} ($0.53 \pm 0.01 \text{ V}$) and ultimately PCE ($1.71 \pm 0.02\%$). The low μ_h of the 77:23 and 42:58 FV:TBTV copolymers (a and d) limited J_{sc} and undercut PCE. Although the PFV homopolymer displayed the highest μ_h , its wide E_g^{opt} diminished light absorption, suppressing J_{sc} , and in turn PCE. Despite its narrow E_g^{opt} , the PTBTV homopolymer device PCE was hindered by both a low μ_h and shallow HOMO level.

Conclusions

A series of statistical D-A copolymers, spanning the composition window from donor homopolymer to acceptor homopolymer, was readily prepared via ADMET polymerization. Optical and electrochemical characterization of the copolymer series reaffirmed the utility of ADMET copolymerization as an ideal means of precisely tuning the electronic structure (e.g., HOMO/LUMO levels and band gap) of D-A copolymers with minimal synthetic effort. Incorporation into polymer-fullerene BHJ solar cells clearly established the direct synthetic tunability of V_{oc} through control of D-A copolymer composition. Integration of the copolymer series into field effect structures elucidated the sensitivity of J_{sc} and FF to variation in the hole mobility of the polymers. Peak photovoltaic performance was found to occur in solar cells based on donor rich statistical D-A copolymers, illustrating the importance of investigating copolymers with non-stoichiometric D-A compositions.

Acknowledgements

This research was funded by the University of Minnesota Initiative for Renewable Energy and the Environment. This

work was also supported partially by the National Science Foundation through the University of Minnesota MRSEC under Award Number DMR-0819885.

Notes and references

^a Department of Chemical Engineering and Materials Science, University of Minnesota, 421 Washington Ave. SE, Minneapolis, MN 55455-0132, USA. E-mail: frisbie@umn.edu

^b Department of Chemistry, University of Minnesota, 207 Pleasant St. SE, Minneapolis, MN 55455-0431, USA. E-mail: hillmyer@umn.edu

^c Department of Chemistry and Biochemistry and Cooperative Institute for Research in Environmental Sciences (CIRES), University of Colorado at Boulder, 216 UCB, Boulder, CO 80309, USA.

† Electronic Supplementary Information (ESI) available: Synthesis details, ¹H NMR spectra, solution UV-vis spectra, cyclic voltammograms, field effect transistor threshold voltage data, and differential scanning calorimetry are included. See DOI: 10.1039/b000000x/

- G. Yu, J. Gao, J. C. Hummelen, F. Wudl and A. J. Heeger, *Science*, 1995, **270**, 1789–1790.
- G. Li, R. Zhu and Y. Yang, *Nature Photon.*, 2012, **6**, 153–161.
- Z. He, C. Zhong, S. Su, M. Xu, H. Wu and Y. Cao, *Nature Photon.*, 2012, **6**, 591–595.
- J. You, C.-C. Chen, Z. Hong, K. Yoshimura, K. Ohya, R. Xu, S. Ye, J. Gao, G. Li and Y. Yang, *Adv. Mater.*, 2013, **25**, 3973–3978.
- J. You, L. Dou, K. Yoshimura, T. Kato, K. Ohya, T. Moriarty, K. Emery, C.-C. Chen, J. Gao, G. Li and Y. Yang, *Nat. Commun.*, 2013, **4**, 1446.
- S.-H. Liao, H.-J. Jhuo, Y.-S. Cheng and S.-A. Chen, *Adv. Mater.*, 2013, **25**, 4766–4771.
- Y. Li, *Acc. Chem. Res.*, 2012, **45**, 723–733.
- H.-J. Jhuo, P.-N. Yeh, S.-H. Liao, Y.-L. Li, Y.-S. Cheng and S.-A. Chen, *J. Chin. Chem. Soc.*, 2014, **61**, 115–126.
- B. Burkhart, P. P. Khlyabich and B. C. Thompson, *Macromolecules*, 2012, **45**, 3740–3748.
- X. Chen, G. L. Schulz, X. Han, Z. Zhou and S. Holdcroft, *J. Phys. Chem. C*, 2009, **113**, 8505–8512.
- C.-H. Chen, C.-H. Hsieh, M. Duboscq, Y.-J. Cheng and C.-S. Hsu, *Macromolecules*, 2010, **43**, 697–708.
- X. Wang, C. Gao, K. Wang, X. Fan, H. Wang, X. Li, Z.-G. Zhang and Y. Li, *J. Polym. Sci. A Polym. Chem.*, 2013, **51**, 4975–4982.
- W. A. Braunecker, S. D. Oosterhout, Z. R. Owczarczyk, N. Kopidakis, E. L. Ratcliff, D. S. Ginley and D. C. Olson, *ACS Macro. Lett.*, 2014, **3**, 622–627.
- B. Burkhart, P. P. Khlyabich, T. C. Canak, T. W. LaJoie and B. C. Thompson, *Macromolecules*, 2011, **44**, 1242–1246.
- P. P. Khlyabich, B. Burkhart, C. F. Ng and B. C. Thompson, *Macromolecules*, 2011, **44**, 5079–5084.
- T. E. Kang, K.-H. Kim and B. J. Kim, *J. Mater. Chem. A*, 2014, DOI: 10.1039/C4TA02426E.
- B. Burkhart, P. P. Khlyabich and B. C. Thompson, *ACS Macro. Lett.*, 2012, **1**, 660–666.
- N. Yamamoto, R. Ito, Y. Geerts and K. Nomura, *Macromolecules*, 2009, **42**, 5104–5111.
- J. C. Speros, B. D. Paulsen, B. S. Slowinski, C. D. Frisbie and M. A. Hillmyer, *ACS Macro Lett.*, 2012, **1**, 986–990.
- M. C. Scharber, D. Mühlbacher, M. Koppe, P. Denk, C. Waldauf, A. J. Heeger and C. J. Brabec, *Adv. Mater.*, 2006, **18**, 789–794.
- Q. Liu, W. Liu, B. Yao, H. Tian, Z. Xie, Y. Geng and F. Wang, *Macromolecules*, 2007, **40**, 1851–1857.
- M. Scholl, S. Ding, C. W. Lee and R. H. Grubbs, *Org. Lett.*, 1999, **1**, 953–956.
- C. W. Bielawski and R. H. Grubbs, *Angew. Chem., Int. Ed.*, 2000, **39**, 2903–2906.
- J. A. Love, J. P. Morgan, T. M. Trnka and R. H. Grubbs, *Angew. Chem., Int. Ed.*, 2002, **41**, 4035–4037.
- Y. Qin and M. A. Hillmyer, *Macromolecules*, 2009, **42**, 6429–6432.
- J. Patel, S. Mujcinovic, W. R. Jackson, A. J. Robinson, A. K. Serelis and C. Such, *Green Chem.*, 2006, **8**, 450–454.
- G. Yang, K. Hu and Y. Qin, *J. Polym. Sci. Part A Polym. Chem.*, 2014, **52**, 591–595.
- N. Yamamoto, R. Ito, Y. Geerts and K. Nomura, *Macromolecules*, 2009, **42**, 5104–5111.
- K. Nomura, H. Morimoto, Y. Imanishi, Z. Ramhani and Y. Geerts, *J. Polym. Sci., Polym. Chem.*, 2001, **39**, 2463–2470.
- J. C. Speros, H. Martinez, B. D. Paulsen, S. P. White, A. D. Bonifas, P. C. Goff, C. D. Frisbie and M. A. Hillmyer, *Macromolecules*, 2013, **46**, 5184–5194.
- Y. He, G. Zhao, J. Min, M. Zhang and Y. Li, *Polymer*, 2009, **50**, 5055–5058.
- I. Jestin, P. Frère, N. Mercier, E. Levillain, D. Stievenard and J. Roncali, *J. Am. Chem. Soc.*, 1998, **120**, 8150–8158.
- B. D. Paulsen and C. D. Frisbie, *J. Phys. Chem. C*, 2012, **116**, 3132–3141.
- V. W. Hultgren, A. W. A. Mariotti, A. M. Bond and A. G. Wedd, *Anal. Chem.*, 2002, **74**, 3151–3156.
- M. J. A. Shiddiky, A. A. J. Torriero, C. Zhao, I. Burgar, G. Kennedy and A. M. Bond, *J. Am. Chem. Soc.*, 2009, **131**, 7976–7989.
- C. M. Cardona, W. Li, A. E. Kaifer, D. Stockdale and G. C. Bazan, *Adv. Mater.*, 2011, **23**, 2367–2371.
- Y. He and Y. Li, *Phys. Chem. Chem. Phys.*, 2011, **13**, 1970–1983.
- D. Veldman, S. C. J. Meskers and R. A. J. Janssen, *Adv. Funct. Mater.*, 2009, **19**, 1939–1948.
- R. A. Street, M. Schoendorf, A. Roy and J. H. Lee, *Phys. Rev. B*, 2010, **81**, 205307.
- R. A. Street, K. W. Song, J. E. Northrup and S. Cowan, *Phys. Rev. B*, 2011, **83**, 165207.
- A. Zen, J. Pflaum, S. Hirschmann, W. Zhuang, F. Jaiser, U. Asawapirom, J. P. Rabe, U. Scherf and D. Neher, *Adv. Funct. Mater.*, 2004, **14**, 757–764.
- P. Schilinsky, U. Asawapirom, U. Scherf, M. Biele and C. J. Brabec, *Chem. Mater.*, 2005, **17**, 2175–2180.
- R. J. Kline, M. D. McGehee, E. N. Kadnikova, J. Liu, J. M. J. Fréchet and M. F. Toney, *Macromolecules*, 2005, **38**, 3312–3319.
- R. C. Hiorns, R. de Bettignies, J. Leroy, S. Bailly, M. Firon, C. Sentein, A. Khoukh, H. Preud'homme and C. Dagron-Lartigau, *C, Adv. Funct. Mater.*, 2006, **16**, 2263–2273.
- J. F. Chang, J. Clark, N. Zhao, H. Sirringhaus, D. W. Breiby, J. W. Andreasen, M. M. Nielsen, M. Giles, M. Heeney and I. McCulloch, *Phys. Rev. B*, 2006, **74**, 115318.
- C. Müller, E. Wang, L. M. Andersson, K. Tvingstedt, Y. Zhou, M. R. Andersson and O. Inganäs, *Adv. Funct. Mater.*, 2010, **20**, 2124–2131.

- 47 R. C. Coffin, J. Peet, J. Rogers and G. C. Bazan, *Nat. Chem.*, 2009, **1**, 657–661.
- 48 J.-H. Huang, F.-C. Chen, C.-L. Chen, A. T. Huang, Y.-S. Hsiao, C. M. Teng, F.-W. Yen, P. Chen and C.-W. Chu, *Org. Electron.*, 2011, **12**, 1755–1762.
- 49 C. Liu, K. Wang, X. Hu, Y. Yang, C.-H. Hsu, W. Zhang, S. Xiao, X. Gong and Y. Cao, *ACS Appl. Mater. Interfaces*, 2013, **5**, 12163–12167.
- 50 B. Qi and J. Wang, *Phys. Chem. Chem. Phys.*, 2013, **15**, 8972–8982.
- 51 L. M. Andersson, C. Müller, C.; B. H. Badada, F. Zhang, U. Würfel and O. Inganäs, *J. Appl. Phys.*, 2011, **110**, 024509.
- 52 M. Svensson, F. Zhang, S. C. Veenstra, W. J. H. Verhees, J. C. Hummelen, J. M. Kroon, O. Inganäs and M. R. Andersson, *Adv. Mater.*, 2003, **15**, 988–991.
- 53 Q. Zhou, Q. Hou, L. Zheng, X. Deng, G. Yu and Y. Cao, *Appl. Phys. Lett.*, 2004, **84**, 1653.
- 54 S. Ko, R. Mondal, C. Risko, J. K. Lee, S. Hong, M. D. McGehee, J. L. Brédas and Z. Bao, *Macromolecules*, 2010, **43**, 6685–6698.
- 55 W. Ma, C. Yang, X. Gong, K. Lee and A. J. Heeger, *Adv. Funct. Mater.*, 2005, **15**, 1617–1622.
- 56 G. Li, V. Shrotriya, J. Huang, Y. Yao, T. Moriarty, K. Emery and Y. Yang, *Nature Mater.*, 2005, **4**, 864–868.
- 57 J. Y. Kim, Y. Qin, D. M. Stevens, O. Ugurlu, V. Kalihari, M. A. Hillmyer and C. D. Frisbie, *J. Phys. Chem. C*, 2009, **113**, 10790–10797.